JOURNAL OF PROPULSION AND POWER
Vol. 13, No. 4, July–August 1997

Effects of Mixing Schemes on Kerosene Combustion in a Supersonic Airstream

M. Owens* and C. Segal†
University of Florida, Gainesville, Florida 32611-2031
and
A. H. Auslender‡
NASA Langley Research Center, Hampton, Virginia 23681-0001

A study of kerosene combustion in a supersonic vitiated airflow at Mach 4.75 flight enthalpy was conducted in direct-connect tests at Mach 1.8 at a stagnation temperature of 1000 K. The effects of shock- and vortex-enhanced mixing mechanisms on the combustion efficiency were evaluated. Also included in this study were the effects of fuel heating and jet penetration. The experimental conditions corresponded to the low end of the hypersonic flight regime. The following geometric configurations were employed: 1) a generic, rearward-facing step, 2) a modified rearward-facing step with beveled edges to facilitate vortex-enhanced mixing, and 3) a rearward-facing wedge (15 or 30 deg) placed downstream of the rearward-facing step to induce shock-enhanced mixing. In all configurations, a gaseous hydrogen–pilot jet was injected parallel to the main flow from the base of the rearward-facing step and the liquid kerosene was injected normal to the main flow at three or five step heights downstream of the step (the step height was 10 mm). Stable kerosene combustion was obtained for a maximum injected kerosene equivalence ratio of 0.86. For efficiency evaluation, the pilot–hydrogen equivalence ratio was selected between 0.02–0.04, while the kerosene equivalence ratio was maintained at 0.325. In all experiments, locally rich stratified kerosene combustion took place in a layer close to the injection wall. The wedge flameholder contributed to an increased kerosene combustion efficiency by the generation of shock–jet interactions. The beveled-edge step improved far-field mixing, thereby reducing the local kerosene equivalence ratio, resulting in the highest kerosene combustion efficiency among all configurations tested. Fuel heating below levels required for flash vaporization (one-third of the flash vaporization energy, in this case) did not contribute to increased combustion efficiency. On the contrary, this level of heating reduced the fuel density with adverse effects on penetration and mixing.

Nomenclature

A = jet exit area
H = step height, 10 mm
$\dot{m}$ = mass flow, rate
P = pressure
q = dynamic pressure ratio
T = temperature
γ = ratio of specific heats for main flow
η = combustion efficiency
ρ = density
ϕ = equivalence ratio

Subscripts
h = hydrogen properties
j/a = jet/air, ratio
k = kerosene properties
s = static properties
0 = stagnation properties
∞ = freestream conditions

Received Sept. 10, 1996; revision received Jan. 20, 1997; accepted for publication March 13, 1997.

*Graduate Research Assistant, Department of Aerospace Engineering, Mechanics, and Engineering Science. Student Member AIAA.

†Assistant Professor, Department of Aerospace Engineering, Mechanics, and Engineering Science. Member AIAA.

‡Aerospace Technologist.

Introduction

THE need to increase the fuel energy–density for hypersonic flight has long been recognized.[1,2] Liquid hydrocarbons are attractive solutions for the low end of the hypersonic flight regime because of their higher volumetric energy content and the relative simplicity of operational logistics.[1,3] In general, the combustion processes in supersonic flows are mixing–limited,[4,5] although a strong mixing–combustion interaction exists, in particular in the flow regions where the Damköhler number is $\mathcal{O}(1)$ (Ref. 6). The difficulties imposed by the use of liquid hydrocarbons, in comparison with gaseous systems, are derived from the longer residence times required for vaporization and the completion of chemical reactions.

Transverse injection provides good penetration and mixing, but at the expense of shock losses[7–11]; therefore, attention has been given to angled injection in the presence of solid[12–16] or aerodynamic ramps.[17] Oblique jets produced by angled injection exhibited less near-field mixing in comparison with transverse injection, but they resulted in good far-field mixing through the generation of large vortical structures. Northam et al.[12] used both an unswept and a swept ramp with angled injection to evaluate the effect of vortex enhanced mixing for a Mach 1.7 hydrogen jet injected in a Mach 2 airstream. The swept ramp induced a higher combustion efficiency than the unswept ramp because of the stronger vortices shed off the ramp that accelerated the mixing processes. The combustion efficiency nearly equaled the mixing performance of transverse injection. Fuller et al.[17] used rows of jets placed at angles to simulate the presence of a physical ramp. This arrangement resulted in a superior near-field mixing compared with the physical ramp for low-momentum ratios and a comparable far-field mixing at high momentum ratios.

In the present study, transverse injection was the primary mode of liquid fuel injection. Both shock–jet interactions and ramp-induced vortex shedding were used to determine the effects of enhanced mixing on the liquid fuel combustion efficiency.

The relatively slower reaction rates of typical liquid hydrocarbons can be accelerated by using a gaseous pilot flame,[18–20] resulting in improved flameholding and increased efficiency. Vinogradov et al.[18] used various combinations of strut and wall injection of both pilot–hydrogen and liquid kerosene to obtain stable combustion at kerosene equivalence ratios as high as 0.6 and pilot equivalence ratios as low as 0.1 for Mach 6 flight conditions. Bonghi et al.[19] evaluated the piloted energy needed to maintain stable combustion of liquid toluene using a rearward-facing step as the main flameholding mechanism with a gaseous hydrogen–pilot flame in a Mach 2.5 airflow. Toluene was selected in that study since it is a component of catalytically cracked methylcyclohexane (MCH). A maximum ratio of the toluene energy content to the pilot energy content was obtained for a given level of piloted energy; beyond that level, the ratio decreased rapidly as a result of liquid fuel enrichment of the recirculation region leading to pilot flame extinction. Kay et al.[20] used a gaseous ethylene pilot to stabilize the combustion of a primary fuel, injected both upstream and downstream of the pilot, for a Mach 3 airflow. Gaseous ethylene was initially used as the primary fuel, achieving combustion efficiencies of 80–100% for overall equivalence ratios up to 0.26. Liquid Jet-A was then used as the primary fuel for equivalence ratios up to 0.07. When injected cold, the Jet-A combustion efficiency was only 25–60%. However, when the liquid Jet-A fuel was heated to conditions of flash vaporization, the Jet-A combustion efficiencies became comparable to those for gaseous ethylene.

Vaporization can be accelerated if liquid fuel is used to cool engine and airframe components, in particular, if the level of heating ensures flash vaporization. A solution may be offered by endothermic fuels that are catalytically cracked during the heating process. It is likely, however, that at the low end of the hypersonic flight regime, the heating level would not be such that flash vaporization can be ensured upon injection, and both liquid and gaseous phases may be present in the fuel.[21] In the present study, partial fuel heating to only one-third of the total energy required for flash vaporization indicated no improvement in the combustion efficiency, with the mixing detrimentally affected because of the reduction in the fuel density resulting in diminished penetration.

In the study presented next, a hydrogen–pilot flame was injected from the base of a rearward-facing step to ignite and maintain a liquid-kerosene-based flame injected normal to the main flow downstream of the step in a Mach 1.8 airstream. This study examined the flameholding ability and the effects of several mixing mechanisms on the combustion efficiency of liquid kerosene, as follows: 1) axial location of the liquid fuel injection, determine the enrichment and the effectiveness of the recirculation region; 2) addition of a wedge between the step and the liquid kerosene injector location, increase mixing via shock-fuel interactions and provide additional recirculation regions; 3) vortex-enhanced mixing via a rearward-facing step with beveled edges, improve the far-field mixing; 4) dynamic pressure ratio of the liquid jet to the freestream flow, dictate the fuel penetration and mixing; and 5) partial heating the liquid kerosene to levels below that required for flash vaporization, determine the tradeoff between accelerated vaporization and chemical reactions vs reduced density and penetration.

Experimental Setup

Figure 1 shows a schematic of the experimental facility, described in detail in Ref. 22. Air is provided from a storage tank to a vitiated, hydrogen-based heater that increases the air stagnation temperature to a maximum of 1200 K. Oxygen replenishment was not available during these experiments, resulting in a vitiated airstream with 16% O_2 mole fraction. The air is then directed via a bellmouth with compression on four sides to a two-dimensional rectangular supersonic nozzle. Six interchangeable, supersonic nozzles are available, thus allowing the entrance Mach number to the test section to be varied from 1.6 to 3.6 with all nozzles ending at the fixed 2.54 × 2.54 cm^2 test section entrance.

The test section, shown in Fig. 2, featured a 10-mm-high rearward-facing step as the main flameholding mechanism. The step included a stagnation chamber from which the pilot flame is generated, parallel to the main flow via three, 1-mm-diam orifices equally spaced in a transverse direction. Two removable injectors were located on the test section wall at 3 and 5H downstream of the step, allowing normal injection of the main fuel. For this study, orifice diameters of 0.5 and 1.0 mm were used. Removable, rearward-facing wedges were attached to the test section wall 2.8H downstream of the step. An oil-based heat exchanger was used to heat the liquid kerosene prior to injection. The onset of thermal choking was delayed by diverging the test section starting 7H downstream of the step with a 3-deg half-angle. Visual access to the test section was provided by quartz windows installed in the three sides of the test section that do not include fuel injection. The test section incorporated 15 pressure ports and 5 thermocouples embedded in the test section wall 0.1 mm below the wetted surface.

Additional pressure transducers and thermocouples were used to measure the experimental conditions, with the kerosene flow rates measured by a turbine flow meter with an accuracy of ±0.5% of the meter reading. A PSI® 9010 Electronic Pressure Scanner with 16 channels and an accuracy of ±0.08% FS (FS = 30 psig) was used to measure simultaneously all test section wall pressures. A National Instruments® SCXI-1000 multiplexer/amplifier was used to collect the temperature data. Data acquisition and experimental control was provided by a

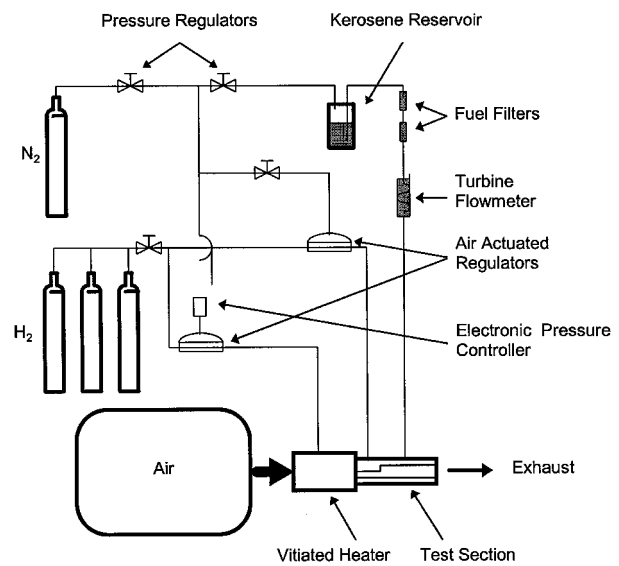

Fig. 1 Facility schematic.

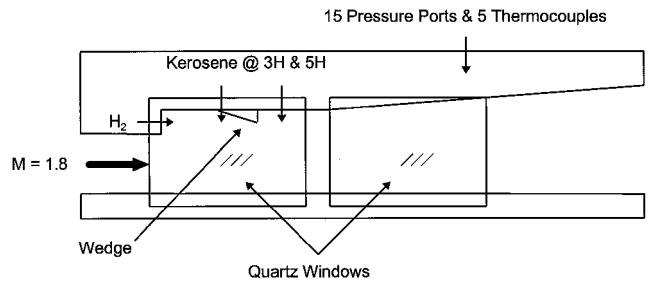

Fig. 2 Test section schematic.

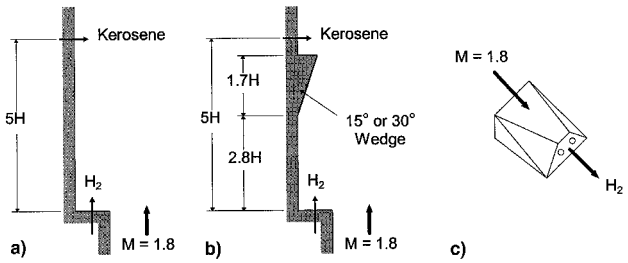

Fig. 3 Mixing schemes: a) baseline, b) shock-inducing wedges, and c) beveled step for vortex-induced mixing.

National Instruments AT-MIO-16E-2 Data Acquisition Board, featuring eight differential input channels and a 500-kHz maximum scan rate installed in a 150-MHz Pentium®-based computer.

Three injection configurations were evaluated in this study (see Fig. 3). Configuration 1 featured a generic rectangular, rearward-facing step. Configuration 2 featured this step with either a 15 or 30 deg wedge installed 2.8H downstream of the step. The length of both wedges was 1.7H. Configuration 3 featured the rearward-facing, beveled-edge step shown in Fig. 3c. The beveled step had the same height (10 mm) as the rectangular step, but the edges parallel to the main flow were beveled to facilitate vortex-enhanced mixing.

Injection Sequence and Analysis

Ignition of the vitiated heater and pilot flame were established at low air pressures, followed by the establishment of the experimental conditions: M_0 = 1.8, P_0 = 430 kPa, T_0 = 1000 K, and an initial pilot equivalence ratio ϕ_h = 0.02. The liquid kerosene was then injected at an equivalence ratio ϕ_k = 0.325. Holding all other parameters constant, the hydrogen–pilot stagnation pressure was then increased to obtain hydrogen–pilot equivalence ratios of 0.028, 0.034, and 0.042, maintaining constant experimental conditions for 5–10 s in each case. It should be noted that in the absence of the pilot flame the combustor flamed out under all of the experimental conditions described here.

Figures 4a–4c show schematics of the combusting flowfield for the three configurations. The airflow underwent expansion around the rearward-facing step where gaseous hydrogen was injected parallel to the main flow and ignited with an electrical discharge. When the pressure rise caused by hydrogen combustion was large enough, the expansion wave around the step turned into a compression shock. At five step heights downstream of the step, liquid kerosene was injected normal to the main flow creating a separation shock upstream of the jet. A weaker reattachment shock (not shown in Fig. 4) was present downstream of the jet. The jet then broke up downstream of the injection site where it vaporized and mixed with the main flow. Inclusion of the wedges generated the shock waves shown in Fig. 4b, and the beveled step induced shedding of counter-rotating vortices as shown in Fig. 4c. Each of these mechanisms interacted in a different way with the fuel jet, as described next.

A one-dimensional, equilibrium chemistry, computer code called DISTORTION_THERMODYNAMICS was used in combination with the experimental data, pressures, and temperatures to obtain the axial liquid kerosene combustion efficiency for each hydrogen–pilot equivalence ratio. The code assumed that the hydrogen–pilot combustion is completed before reaching the liquid fuel injection station and, thus, prescribes the fluid thermochemical conditions at this station as resulting from the hydrogen equilibrium calculation. The code then assumed a one-step instantaneous cracking of the kerosene fuel into a mixture of gaseous methane and gaseous ethylene by modeling kerosene as dodecane, via the following reaction:

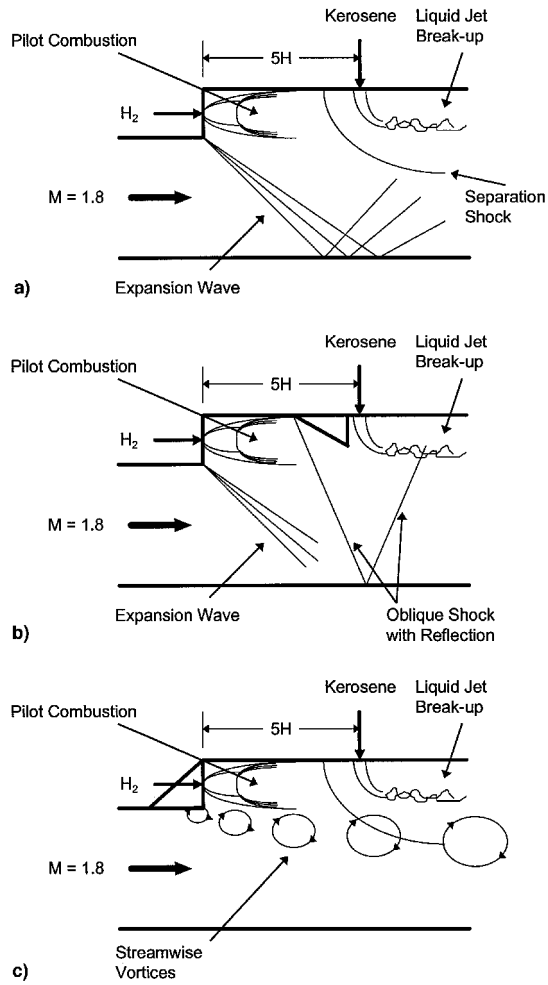

Fig. 4 Combusting flowfield schematic: a) baseline, b) baseline with wedge, and c) beveled-step configurations.

$$C_{12}H_{26} \rightarrow CH_4 + 5.5C_2H_4 \quad (1)$$

Adjustments were made in the energy balance to account for the differences in the heats of formation of the species in Eq. (1) and in the heat of vaporization of the liquid kerosene. The methane was assumed to be completely combusted, while the ethylene was allowed to burn as necessary to match the pressure boundary conditions obtained from the experimental data. The percentage of unreacted carbon at the exit of the duct is taken to be the combustion efficiency of the liquid kerosene. This calculation represents a major simplification of the physics of the flow and cannot, therefore, describe in detail the complex processes of jet breakup, vaporization, mixing, and the complex finite rate chemistry present in this environment that is dominated by shock waves and strong spatial gradients. It offers, nevertheless, a simplified algorithm by which measured parameters (wall pressure and temperatures) can be used with minimal computational effort to predict trends as various thermoaerodynamic and geometrical parameters are changed.

Results

Effect of Axial Kerosene Distribution

Kerosene was injected at both the 3 and 5H axial locations downstream of the rearward-facing step via a 0.5-mm-diam orifice. With kerosene injection at the 3H location, large amounts of liquid kerosene were entrained into the recirculation region created by the step, quenching the pilot flame. This

was noticed even when the kerosene equivalence ratio was reduced below 0.1. Only when the jet penetration was increased by reducing the orifice diameter to 0.2 mm, thereby increasing the jet/air dynamic pressure ratio by more than an order of magnitude, could a stable flame be maintained. In sharp contrast were the results with the kerosene injection at the 5*H* axial location downstream of the step. In these cases, kerosene combustion was stable even with kerosene equivalence ratios as high as 0.86 and with an orifice diameter of 1.0 mm. This injection site was practically outside the boundaries of the recirculation region; thus, only small amounts of liquid reached the pilot flame recirculation region and the pilot flame could be sustained. All of the results presented next were further obtained with a constant kerosene equivalence ratio of 0.325, injected at the 5*H* axial location downstream of the step.

Effect of Hydrogen–Pilot Equivalence Ratio

Previous studies investigated the benefits of using a gaseous pilot flame to stabilize the combustion of liquid hydrocarbon fuels.[18–20] The optimum strength of the pilot flame is derived from the tradeoff between the need to maximize the volumetric energy content of the combined combustion system by using the lowest possible hydrogen–pilot equivalence ratio and the need to maximize the combustion efficiency of the liquid hydrocarbon fuel.

Figure 5 shows the test section axial wall pressure distribution, normalized by the test section entrance static pressure, for the baseline configuration. The parameter in this plot is the hydrogen–pilot equivalence ratio. Because of expansion, the pressure behind the step drops 60% of the inlet static pressure. After reattachment the pressure increases as the shock waves and heat release contribute to the Mach number reduction. The kerosene combustion efficiency (shown in Fig. 6 as calculated from the code) were on the order of 57% for all hydrogen–pilot equivalence ratios. The visual images showed a stratified combustion region for the liquid kerosene, which indicated that while the global kerosene equivalence ratio was only 0.325, the local kerosene equivalence ratio in the combustion region was much higher. Initially, for low ϕ_h, the kerosene combustion efficiency increases because of heat addition; however, following a maximum, the efficiency indicates a low rate decay. The decreasing kerosene combustion efficiencies were attributed to continuing enrichment of the burning region confined near the injection wall.

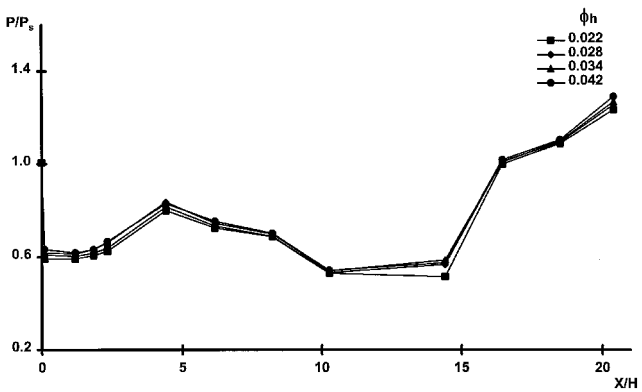

Fig. 5 Axial wall pressure distribution for the baseline configuration with kerosene combustion.

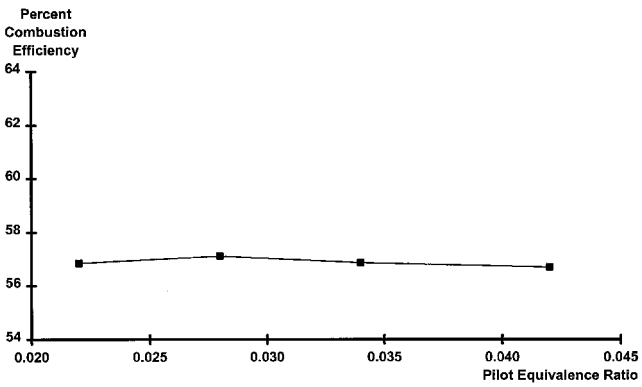

Fig. 6 Kerosene combustion efficiency for the baseline configuration (f_K = 0.325).

Effect of the Shock–Jet Interactions

Wedges were added as shown in Fig. 3b to produce oblique shocks that would improve kerosene jet breakup and mixing. In addition, the wedges created a cavity in which the hydrogen–pilot flame was separated from the liquid kerosene. The addition of the wedges changed the flowfield significantly, producing shock waves that reflected from the test section opposite wall and interacted with the near-field jet breakup and mixing region. This interaction is substantially stronger than the effect of the reflections from the expansion waves from the step. The effect is different than the far-field mixing enhancement resulting from the counter-rotating vortices produced off the beveled-edged step. It should be noted that the multiple shock–jet interactions are dependent on the height of the channel and would affect the jet mixing region with a different intensity in a differently sized duct.

When the wedge was placed too close to the step (i.e., 0.8*H*), it reduced the volume of the cavity in which the pilot flame combusted, resulting in a locally rich region and leading to the extinction of the hydrogen–pilot flame for $\phi_h > 0.015$. When the wedge was moved downstream to the 2.8*H* location, the pilot flame was stable for all hydrogen–pilot equivalence ratios used in these experiments.

The benefit of the addition of the wedge flameholder was evidenced by the increased kerosene combustion efficiency

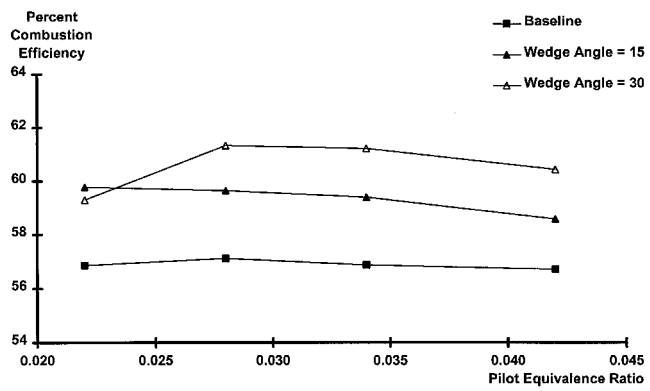

Fig. 7 Kerosene combustion efficiency for the 15- and 30-deg wedges. The baseline configuration is shown for comparison (f_K = 0.325).

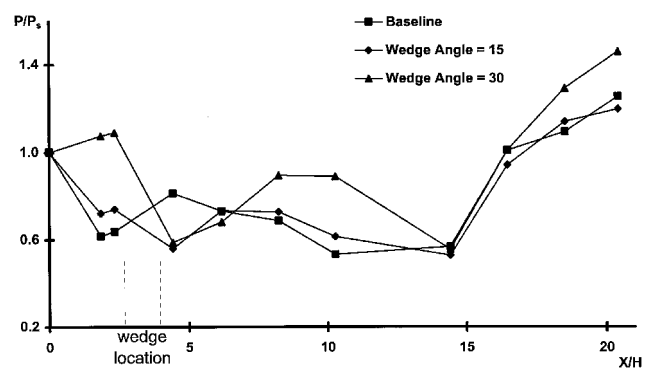

Fig. 8 Axial wall pressure distribution for the wedge configurations. The baseline configuration is shown for comparison (f_H = 0.028).

(Fig. 7). The 15-deg wedge resulted in a 2-percentage-points increase and the 30-deg wedge resulted in a 4-percentage-points increase in the kerosene combustion efficiency over the baseline configuration. Figure 8 shows a comparison of the axial wall pressure distribution of the wedge configurations with the baseline configuration. The pressure rise measured immediately upstream of the 15-deg wedge indicates the separation induced by the formation of the shock wave at the wedge leading edge. In the base, downstream of the wedge, pressure decreases as a result of the expansion at the wedge's corner. In the far region, beyond $6H$, the pressure distribution with the 15-deg wedge is similar to the baseline configuration. The 30-deg wedge indicates a stronger effect, due probably to the detachment of the shock formed at its leading edge and a reduction of the effective size of the recirculation region. The strength of this shock is evident in the reflections measured between $8-10H$.

Effect of Vortex-Enhanced Mixing

Northam et al.[12] used a swept ramp with parallel injection on the downstream side of the wedge to enhance the combustion efficiency of a fuel injected parallel to the main flow. The swept ramp showed a higher combustion efficiency than the unswept ramp. The generic, rearward-facing step was replaced in this study by a rearward-facing step with the edges parallel to the main flow beveled (see Fig. 3c). These beveled-edges created counter-rotating vortices that enhanced the entrainment of the fuel into the core of the airstream, improving the mixing.

Figure 9 shows the axial wall pressure for kerosene combustion with both the baseline and the beveled-edge steps. The beveled step produces three dimensional expansions that reflect from the wind-tunnel sidewalls and result in the pressure rise seen in the figure in the vicinity of the step. The beveled-edge step has a significant effect on the combusting flowfield as evidenced by the sharp pressure rise in the far field, beyond $15H$, where substantial heat is released because of improved mixing. The beveled-edge step yielded higher kerosene combustion efficiencies (as shown in Fig. 10) than any other configuration tested here (63%).

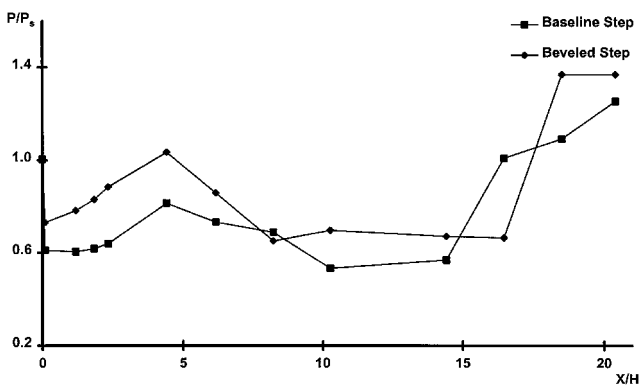

Fig. 9 Axial wall pressure distribution for kerosene combustion with the baseline step and the beveled-edge step ($f_H = 0.028$).

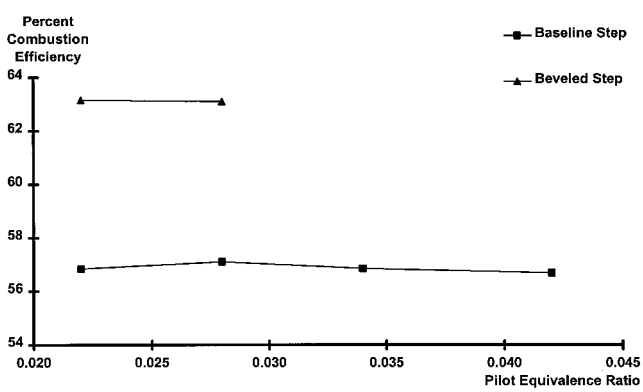

Fig. 10 Kerosene combustion efficiency for the baseline step and the beveled-edge step ($f_K = 0.325$).

Effect of Dynamic Pressure Ratio

It was shown in previous works[23] that the jet penetration scaled approximately with the square root of the dynamic pressure ratio $q_{j/a}$ of the liquid jet to the freestream flow, with $q_{j/a}$ defined as

$$q_{j/a} = \frac{(\dot{m}_k^2/\rho_k A_k^2)}{\gamma P_\infty M_\infty^2} \tag{2}$$

Visual measurements of the width of the stratified kerosene combustion region indicated that the penetration indeed follows the same scaling. For the experiments discussed thus far, with a kerosene injector diameter of 0.5 mm and a kerosene equivalence ratio of 0.325, the dynamic pressure ratio of the liquid jet to the freestream air obtained from Eq. (2) was 2.5. To determine the effect of the liquid jet penetration on the liquid kerosene combustion efficiency, a 1.0-mm injector was used with the baseline configuration and the same kerosene equivalence ratio, resulting in a dynamic pressure ratio of only 0.2.

The calculated kerosene combustion efficiencies are shown in Fig. 11 for both the 0.5-mm injector (the baseline configuration) and the 1.0-mm injector. Results indicated that kerosene combustion efficiency for the 1.0-mm injector was much more sensitive to the hydrogen–pilot equivalence ratio than for the 0.5-mm injector. This is because of the higher kerosene equivalence ratios in a narrower combustion region near the injection wall as a result of reduced penetration. While the kerosene combustion efficiency for the 1.0-mm injector was higher for the lower hydrogen–pilot equivalence ratios, because of the increased residence time of the liquid fuel in the recirculation region, it decreased much more sharply with increasing hydrogen–pilot equivalence ratio than did the 0.5 mm, eventually dropping to levels below those obtained with the 0.5-mm injector.

The reduced jet penetration also had a noticeable effect on the wall temperatures. The time histories of the wall temperature $8.1H$ downstream from the step ($3.1H$ downstream from the injector) are shown in Fig. 12 for both injector diameters. Figure 12 indicates that liquid film cooling was present for both conditions. However, the local cooling was more severe for the case of low penetration. It should be noted that the time origin in Fig. 12 is arbitrary; thus, the liquid injection occurred at different times during the test section wall warm up.

Effect of Heating the Fuel Below the Levels Required for Flash Vaporization

At hypersonic cruise, it is anticipated that liquid fuels will be heated to flash vaporization by using the fuel to cool engine

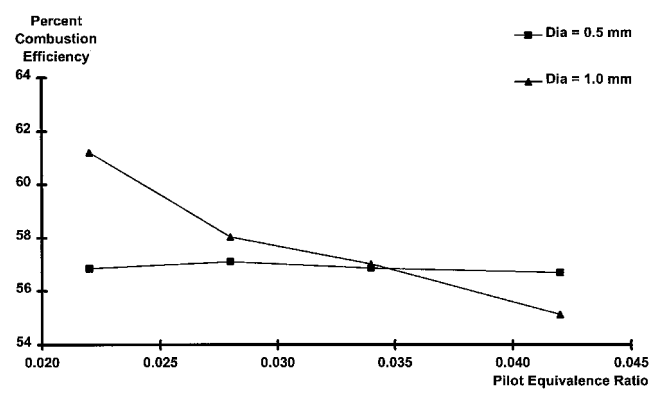

Fig. 11 Kerosene combustion efficiencies for the 0.5-mm injector (the baseline configuration) and the 1.0-mm injector ($f_K = 0.325$).

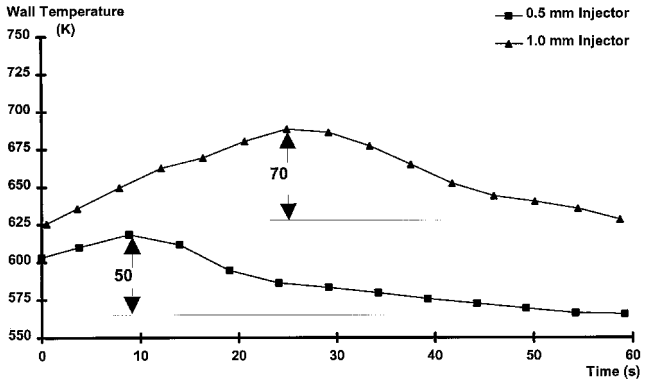

Fig. 12 Wall temperature time histories at the 8.1*H* station, downstream of the liquid kerosene injection site, for both the 0.5- and 1.0-mm injectors.

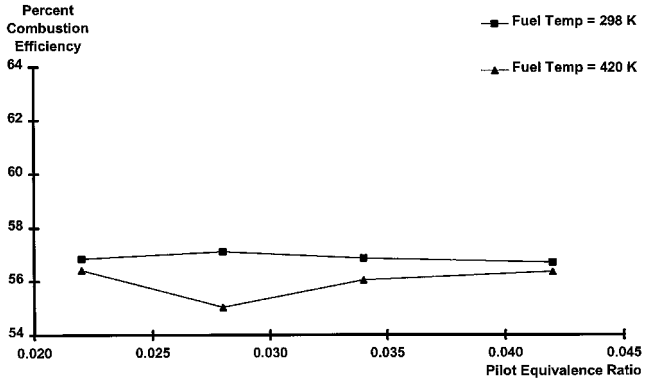

Fig. 13 Kerosene combustion efficiency for the 298 K fuel (the baseline configuration) and the 420 K fuel ($f_K = 0.325$).

and airframe components prior to injection. Kay et al.[20] examined the effects of heating the liquid hydrocarbon fuel to flash vaporization and indicated that combustion efficiencies comparable with gaseous fuel can be achieved. However, there may be situations for which the fuel will be heated to levels significantly below those required for flash vaporization, in particular during cold starts. In this study, only one-third of the energy required for flash vaporization was supplied to the fuel, resulting in a stagnation temperature for the liquid kerosene of 420 K at the given experimental conditions. The baseline configuration was employed for this case.

Figure 13 shows the kerosene combustion efficiency evaluated for both heated and unheated fuel. It was estimated that the lower density of the heated fuel reduced the jet penetration and resulted in a higher kerosene equivalence ratio in the stratified kerosene combustion region leading to a reduction of the kerosene combustion efficiency. The low levels of heating were not sufficient to accelerate the vaporization and chemical reactions to a significant degree in this case, as flash vaporization would.

Summary and Conclusions

This study examined the effects of selected mixing schemes on the liquid kerosene combustion efficiency and the effect of partial fuel heating.

The results indicated the following:

1) Kerosene injection directly into the recirculation region resulted in quenching of the pilot flame. Liquid fuel injection downstream of that region maintained the flame up to equivalence ratios of 0.86.

2) The kerosene combustion efficiency for the baseline configuration was approximately 57%. As the pilot flame equivalence ratio increases there is an initial increase in the kerosene combustion efficiency followed by a slight decreasing trend because of the formation of a fuel-rich stratified layer in the vicinity of the injection wall.

3) The wedge angle had a significant effect on the kerosene combustion efficiency as it increased the interactions between the shock waves and the rich burning layer. The kerosene combustion efficiency increased with the wedge angle, 2 percentage points for the 15-deg wedge and 4 percentage points for the 30-deg wedge over the baseline efficiency. The intensity of the shock-wave–jet interactions depend on the internal geometry of the channel and are likely to differ in a differently sized duct.

4) The vortex-enhanced mixing in the far field generated by the use of the beveled-edge step yielded the highest kerosene combustion efficiency of all configurations tested, i.e., 6 percentage points above the baseline.

5) The kerosene combustion efficiencies obtained for the 1.0-mm injector (low dynamic pressure) were much more sensitive to the hydrogen–pilot equivalence ratio, sharply decreasing with increasing hydrogen–pilot equivalence ratio. At low hydrogen–pilot equivalence ratios, 0.02, the kerosene combustion efficiency was high because of the increased residence time of the liquid fuel in the burning region.

The lower density of the heated fuel reduced the jet penetration, which resulted in a reduction of the kerosene combustion efficiency. This effect was stronger than the acceleration of the vaporization and chemical kinetics rates.

References

[1]Billig, F. S., "Research on Supersonic Combustion," *Journal of Propulsion and Power*, Vol. 9, No. 4, 1993, pp. 499–514.

[2]Waltrup, P. J., "Liquid-Fueled Supersonic Combustion Ramjets: A Research Perspective," *Journal of Propulsion and Power*, Vol. 3, No. 6, 1987, pp. 515–524.

[3]Karagozian, A. R., "Fuel Injection and Flameholding in High Speed Combustion Systems," *Major Research Topics in Combustion*, Springer–Verlag, 1992, pp. 237–252.

[4]Brescianini, C. P., and Morgan, R. G., "An Investigation of a Wall-Injected Scramjet Using a Shock Tunnel," AIAA Paper 92-3965, July 1992.

[5]Gruber, M. R., Nejad, A. S., Chen, T. H., and Dutton, J. C., "Mixing and Penetration Studies of Sonic Jets in a Mach 2 Freestream," *Journal of Propulsion and Power*, Vol. 11, No. 2, 1995, pp. 315–323.

[6]Segal, C., McDaniel, J. C., Whitehurst, R. B., and Krauss, R. H., "Mixing and Chemical Kinetics Interactions in a Mach 2 Reacting Flow," *Journal of Propulsion and Power*, Vol. 11, No. 2, 1995, pp. 308–314.

[7]Schetz, J. A., and Billig, F. S., "Penetration of Gaseous Jets Injected into a Supersonic Stream," *Journal of Spacecraft and Rockets*, Vol. 3, No. 11, 1966, pp. 1658–1665.

[8]Schetz, J. A., Hawkins, P. F., and Lehman, H., "Structure of Highly Underexpanded Transverse Jets in a Supersonic Stream," *AIAA Journal*, Vol. 5, No. 5, 1967, pp. 882–884.

[9]Schetz, J. A., Weinraub, R. A., and Mahaffey, R. E., Jr., "Supersonic Transverse Injection into a Supersonic Stream," *AIAA Journal*, Vol. 6, No. 5, 1968, pp. 933, 934.

[10]Mays, R. B., Thomas, R. H., and Schetz, J. A., "Low Angle Injection into a Supersonic Flow," AIAA Paper 89-2461, July 1989.

[11]Fuller, E. J., Thomas, R. H., and Schetz, J. A., "Mixing Studies of Helium in Air at High Supersonic Speeds," *AIAA Journal*, Vol. 30, No. 9, 1992, pp. 2224–2243.

[12]Northam, G. B., Greenburg, I., Byington, C. S., and Capriotti, D. P., "Evaluation of Parallel Injector Configurations for Mach 2 Combustion," *Journal of Propulsion and Power*, Vol. 8, No. 2, 1992, pp. 491–499.

[13]Hartfield, R. J., Hollo, S. D., and McDaniel, J. C., "Experimental Investigation of a Supersonic Swept Ramp Injector Using Laser-Induced Iodine Fluorescence," *Journal of Propulsion and Power*, Vol. 10, No. 1, 1994, pp. 129–135.

[14]Schetz, J. A., and Swanson, R. C., "Turbulent Jet Mixing at High Supersonic Speeds," *Zeitschrift Für Flugwissenschaften*, Vol. 21, No. 1, 1973, pp. 166–173.

[15]Tillman, T. G., Patrick, W. P., and Patterson, R. W., "Enhanced Mixing of Supersonic Jets," *Journal of Propulsion and Power*, Vol. 7, No. 6, 1991, pp. 1006–1014.

[16]Yang, J., Kubota, R., and Zukoski, E. E., "A Model for Characterization of a Vortex Pair Formed by Shock Passage over a Light Gas Inhomogeneity," *Journal of Fluid Mechanics*, Vol. 258, Jan. 1994, pp. 217–244.

[17]Fuller, R. P., Wu, P. K., Nejad, A. S., and Schetz, J. A., "Fuel-Vortex Interactions for Enhanced Mixing in Supersonic Flow," AIAA Paper 96-2661, July 1996.

[18]Vinogradov, V., Kobigsky, S., and Petrov, M., "Experimental Investigation of Liquid Carbon-Hydrogen Fuel Combustion in Channel at Supersonic Velocities," AIAA Paper 92-3429, July 1992.

[19]Bonghi, L., Dunlap, M. J., Owens, M., Young, C. D., and Segal, C., "Hydrogen Piloted for Supersonic Combustion of Liquid Fuels," AIAA Paper 95-0730, Jan. 1995.

[20]Kay, I. W., Peschke, W. T., and Guile, R. N., "Hydrocarbon-Fueled Scramjet Combustor Investigation," *Journal of Propulsion and Power*, Vol. 8, No. 2, 1992, pp. 507–512.

[21]Petley, D. H., and Jones, S. C., "Thermal Management for a Mach 5 Cruise Aircraft Using Endothermic Fuel," *Journal of Aircraft*, Vol. 29, No. 3, 1992, pp. 287–298.

[22]Segal, C., and Young, C. D., "Development of an Experimentally Flexible Facility for Mixing-Combustion Interactions Studies in Supersonic Flow," *Journal of Energy Resources Technology*, Vol. 118, June 1996, pp. 152–158.

[23]Arai, T., and Schetz, J. A., "Injection of Bubbling Liquid Jets from Multiple Injectors into a Supersonic Stream," *Journal of Propulsion and Power*, Vol. 10, No. 3, 1994, pp. 382–386.